J Appl Electrochem (2012) 42:561–571
DOI 10.1007/s10800-012-0431-3

ORIGINAL PAPER

Zn–Sn electrodeposition from deep eutectic solvents containing EDTA, HEDTA, and Idranal VII

Nuno M. Pereira · Sónia Salomé · Carlos M. Pereira · A. Fernando Silva

Received: 31 January 2012 / Accepted: 5 May 2012 / Published online: 31 May 2012

Abstract The use of deep eutectic solvents for metal electrodeposition has become an area of interest in the recent years. In this study, ethaline, propeline, and reline were used as solvents for the electrodeposition of Sn–Zn alloys. Ethaline, propeline, and reline displayed identical voltammetric profiles for the reduction of Zn(II) and Sn(II). Further studies were carried out in ethaline which is the liquid with lowest viscosity. To improve physical and morphological properties of the Sn–Zn deposits, additives were added to the ionic liquid solution. In this study, the addition of three chelators (EDTA, HEDTA, and Idranal VII) and their effects on the voltammetric behavior of zinc and tin and the resultant morphology was described. The structure and composition of the Zn–Sn deposit was largely affected by the additives with the largest effect being obtained in the presence of Idranal VII.

Keywords Electrodeposition · Deep eutectic solvent · Sn–Zn alloy · Additives

1 Introduction

The metal finishing industry throughout the world has a continuing desire to obtain sacrificial plated coatings that provide even higher standards of protection [1] and Sn–Zn alloys with the appropriate composition are a viable alternative to cadmium [2]. Such alloys offer high corrosion protection for steel, good frictional properties and ductility after plating, and good solderability. They also have low electrical contact resistance and are not subject to bimetallic corrosion [3].

The properties of the coatings are strongly related to the morphological and structural characteristics of the deposits that depend on the operating conditions, nature of additive added, mode of current applied, etc. [4].

The generic term "plating additives" covers a wide variety of chemicals which affect the deposits in different ways [5]. The additives can be organic, metallic, ionic, or nonionic, can adsorb at the plated surface and often are incorporated in the deposit. The use of additives in the electrodeposition solution is extremely important due to their influence on the structure and growth of the resulting deposit. It has been shown that the presence of additives influences the physical and mechanical properties of electrodeposits such as grain size, brightness, internal stress, pitting, and even chemical composition [6].

Additives are frequently assumed to act as catalysts or inhibitors of the electrodeposition process by promoting the complexation of the metal ions and/or raising the activation polarization of single ions by blocking the active sites on the substrate [5].

When the reduction potentials of two metals are far apart, their co-deposition is difficult. In general, it is necessary the application of high overpotentials which leads to dendritic deposits [7]. An ideal co-deposition bath should deposit all the elements at a single or in a narrow range of potentials [8]. For the Sn–Zn system, a large potential difference is observed in the reduction potential so it is necessary to add appropriate chelating agents to bring the deposition potentials closer.

N. M. Pereira · S. Salomé · C. M. Pereira · A. Fernando Silva (✉)
CIQ-L4, Departamento de Química e Bioquímica, Faculdade de Ciências, Universidade do Porto, 4169-007 Porto, Portugal
e-mail: afssilva@fc.up.pt

C. M. Pereira
e-mail: cmpereir@fc.up.pt

Table 1 Composition of the DES used

DES	Reagents	Ratio	Viscosity η (cP)
Ethaline	Choline chloride:ethylene glycol	1 ChCl:2 EG	36
Propeline	Choline chloride:1,2-propylene glycol	1 ChCl:2 PG	89
Reline	Choline chloride:urea	1 ChCl:2 U	632

Almost the entire electroplating sector is currently based on aqueous solution generally acid or basic, and containing cyanide [9–11]. Due to the toxicity of these baths and the difficulty to control parameters, alternative baths have been investigated using different aqueous baths containing different additives [2, 3, 12, 13].

A green alternative for the electrodeposition baths is the use of room-temperature ionic liquids, RTILs [14, 15]. RTILs have many favorable properties such as negligible vapor pressure at elevated temperature, high ionic conductivity, good thermal stability, and wide electrochemical window [14, 15]. The industrial use of RTILs is not yet generalized due to the high cost and the difficulty in handling such liquids. For ionic liquids to be used efficiently in the industrial processes, they should be economically viable, simple to handle, and recyclable. An alternative class of ionic liquids, called deep eutectic solvent (DES), based on combinations of choline chloride with hydrogen bond donors, such as ethylene glycol (EG), was investigated by Abbott et al. [16–18] and by Whitehead et al [19]. These eutectic mixtures have properties similar to RTILs but they are cheap, easily handled, and environmental friendly [18, 20].

This work presents the first study on the effect of a group of additives, which have complexing properties, on the electrodeposition of tin and zinc from a DES formed by choline chloride and EG (ethaline). In this study, we have studied the effects of three similar aminopolycarboxylate ligands, *N*-(2-hydroxyethyl)ethylenediamine-*N*,*N*′,*N*′-triacetic acid trisodium salt (Idranal VII, also known as HEDTA-Na_3), *N*-(2-hydroxyethyl)ethylenediamine-*N*,*N*′,*N*′-triacetic acid (HEDTA), and Ethylenedinitrilotetraacetic acid (EDTA) in the deposition of tin and tin–zinc alloys using ethaline as an electroplating bath. The influence of the additives was examined by voltammetry and the deposits obtained under potentiostatic conditions were examined by scanning electron microscopy (SEM).

2 Experimental

Choline chloride ($HOC_2H_4N(CH_3)_3Cl$) (ChCl) (Aldrich 99 %) was dried overnight at 60 °C before use. EG (Aldrich 99.8 %), EDTA (Sigma, 99 %), HEDTA (Fluka, ≥98 %), Idranal VII (Riedel, 99 %), tin chloride (Fluka 97.0 %), and zinc chloride (Fluka 98.0 %) were used as received. The eutectic mixtures were formed at 75 °C until a homogeneous colorless liquid was obtained, by stirring the ChCl with the hydrogen bond donor as resumed in Table 1 [21].

The electrochemical experiments were carried out in a three-electrode glass cell with a platinum electrode (Pt) (Metrohm, 2 mm diameter) as working electrode, a platinum mesh as counter electrode, and a calomel electrode filled with a saturated aqueous choline chloride solution (CE(ChCl)) as reference electrode. All the potentials were reported with respect to this reference. The working electrode was polished with a 3 μm diamond paste, rinsed thoroughly with Millipore water, sonicated for 5 min, and dried with nitrogen. The voltammetric studies were carried out using an Autolab PSTAT10 potentiostat controlled with GPES 4.8 software and the voltammograms were performed at 75 °C under nitrogen atmosphere.

The electrodeposited films were prepared at −1.7 V (vs. CE(ChCl)) without stirring, at 75 °C. The samples were then thoroughly rinsed in Millipore water and dried using a flow of nitrogen. Surface analysis was carried out using the SEM FEI Quanta 400 FEG/EDAX Genesis X4M property of CEMUP.

The current efficiency (CE) of the electrodeposition process was assessed as the ratio between the cathodic (Q_c) and anodic (Q_a) charges from the cyclic voltammograms [3, 12, 22].

3 Results

3.1 Effect of the hydrogen bond donors constituting the liquid

Figure 1a–c shows a comparison of the cyclic voltammograms obtained with ethaline, propeline, and reline solutions containing $ZnCl_2$ and $SnCl_2$. It is clear that the nature of the liquid does not have any significant influence on the voltammetric profile of Zn (II) and Sn (II) in the solution. The noticeable variation is essentially on the value of the peak current density, which may be attributed to the difference on the viscosity of the liquid [23]. The peak current is lower for the deposition in reline which is the liquid with higher viscosity (Table 1). The voltammetric profile in

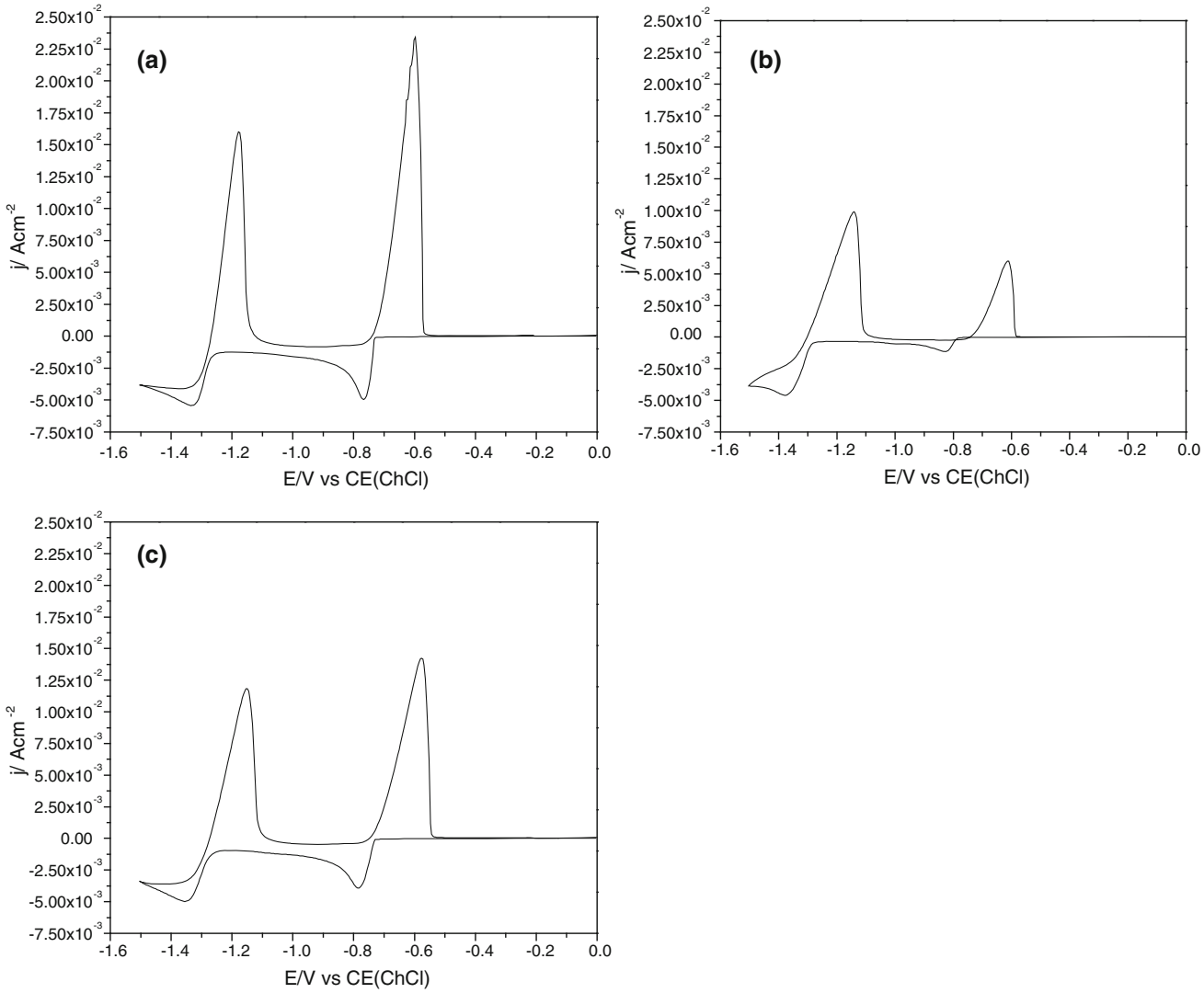

Fig. 1 Cyclic voltammograms for 2.7×10^{-1} M of $ZnCl_2$ and 5.8×10^{-2} M of $SnCl_2$ in a solution of **a** ethaline, **b** reline, **c** propeline using a Pt disk at 75 °C at 50 mVs^{-1}

Fig. 1 is similar to those reported by Abbott et al [18] for the negative going scan, but differs in the oxidative scan since our data only shows one oxidation peak corresponding to the tin oxidation.

The peak potentials are almost invariant with the nature of the ligand suggesting that the deposition occurs from the same species in the solution. Indeed, analyzing the EXAFS data, Abbott et al. [24] discovered that $[ZnCl_4]^{2-}$ is the predominant zinc ion in both reline and ethaline. Contrasting with earlier results from FAB experiments which suggested the presence of several other species, some of which of cationic nature [18]. For Sn, there is not yet EXAFS information but it may be admissible to consider the predominance of $[SnCl_4]^{2-}$ despite the information from FABS that suggests a mixture of $[SnCl_3]^-$ and $[Sn_2Cl_5]^-$ [18].

Since the voltammetric profile of zinc and tin is obtained with the three liquids were identical further studies were carried out in ethaline which is the liquid with lowest viscosity.

3.2 Effect of additives on the deposition of Zn and Sn from ethaline

3.2.1 Zinc deposition

Figure 2 compares the cyclic voltammetric response of a solution of ethaline containing 5.5×10^{-1} M of $ZnCl_2$ in absence of chelators (a) and in the presence of different chelators, (b) EDTA, (c) HEDTA, and (d) Idranal VII.

The onset of the Zn (II) reduction occurs at $E = -1.09$ V with a reduction peak at $E_{p\ red.} = -1.33$ V, the

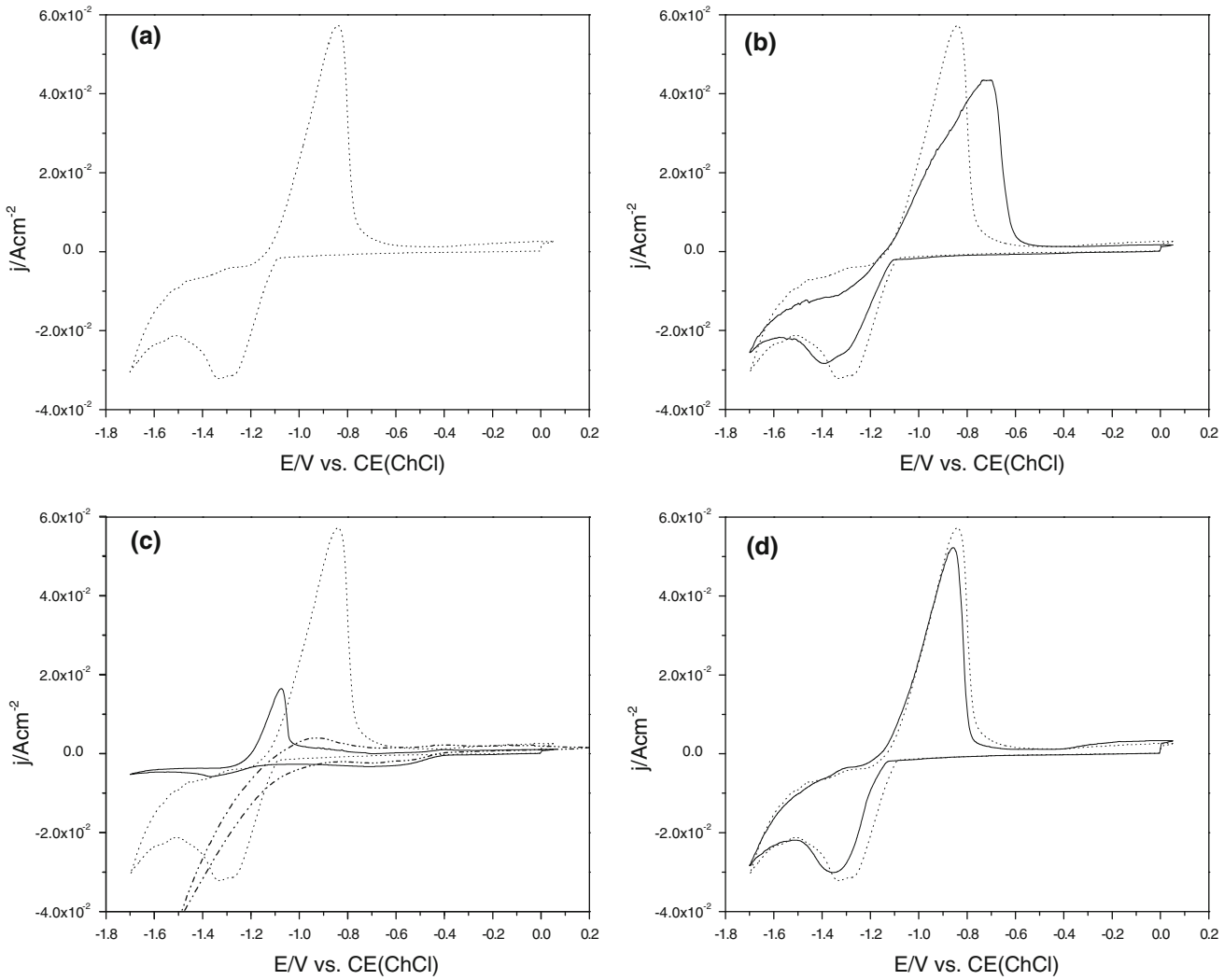

Fig. 2 Cyclic voltammograms for 5.5×10^{-1} M of $ZnCl_2$ (**a**) and with the following additives: **b** saturated solution of EDTA, **c** 5.5×10^{-2} M of HEDTA, **d** 5.5×10^{-2} M of Idranal VII using a Pt disk at 75 °C at 50 mVs^{-1} immersed in ethaline. The *dashed lines* in (**b**–**d**) represent the voltammograms obtained in the absence of additives (**a**). The *dash-dot-dash line* in (**c**) represents the voltammogram obtained for HEDTA and ethaline solution

oxidation of zinc originates only one peak at $E_{p\ ox.} = -0.84$ V.

In the absence of chelators, the observation of two poorly resolved deposition peaks may be taken as indication of the formation of two distinct Zn deposits [23]. However, the deposition from two distinct zinc species in solution may not be completely ruled out despite EXAFS information [24]. Indeed, EXAFS spectra were obtained and late fitted for an ethaline solution containing 0.3 M of $ZnCl_2$, while the voltammetric experiments were carried out for ethaline solution containing 0.55 M of $ZnCl_2$. The oxidative profile of removal the zinc deposits show no indication of the existence of two distinct Zn deposits or the formation of two different zinc species.

It is clear from Fig. 2b–d that the presence of the chelators causes significant changes on the shape of the voltammograms and on the peak position. In the presence of EDTA (Fig. 2b), the onset of the Zn (II) reduction is nearly unchanged when compared with that obtained in the absence of additives but the reduction profile is shifted to more negative potentials ($E_{p\ red.} = -1.39$ V). It should be emphasized that the reduction profile in the presence of EDTA also shows two peaks but better resolved. The anodic scan shows a peak positively shifted that corresponds to the zinc removal ($E_{p\ ox.} = -0.72$ V) with a shoulder on the rising part which is not visible in the absence of EDTA. The presence of EDTA apparently allows to discriminate the possible existence of two energetically different phases of zinc deposited [23] or the deposition of zinc from two different species in solution which are stripped at different potentials and therefore the existence of a Zn–EDTA species cannot be ruled out

[7, 25]. Therefore, the peak occurring at more negative potentials could be originated by the deposition of zinc from Zn–EDTA species.

The presence of HEDTA has the largest effect on the voltammetric response (Fig. 2c). The reduction current starts at more negative potentials ($E_{p\ red.} = -1.19$ V) and remain low in the whole potential range (5× lower than the reduction current in the absence of chelator). The extent of the zinc deposition is lower than in the absence of HEDTA as indicated by the small oxidation peak which occurs at more negative potentials ($E_{p\ ox.} = -1.07$ V).

The presence of Idranal VII in the $ZnCl_2$ solution originates cyclic voltammetric profiles practically identical to those obtained with the additive-free solution (Fig. 2d). Only a small shift of the peak potentials is detected (~ -25 mV) and only one reduction peak is observed.

3.2.2 Tin deposition

Similar experiments were carried out for an ethaline solution containing $SnCl_2$. The onset of Sn (II) reduction occurs at $E = -0.6$ V with a reduction peak at $E_{p\ red.} = -0.71$ V. The removal of the tin deposit occurs with a formation of one oxidation peak at $E_{p\ ox.} = -0.42$ V. The presence of either EDTA or HEDTA (Fig. 3b, c) does not change the general features of the CVs. In contrast to what was observed in the deposition of zinc, where the presence of HEDTA significantly reduces the zinc deposition. In the case of tin, its deposition is promoted by the presence of HEDTA. Major effects are observed when Idranal VII (Fig. 3d) is added to the solution, namely the Sn (II) reduction is largely shifted to more negative potentials although a small reduction peak is detected at the same

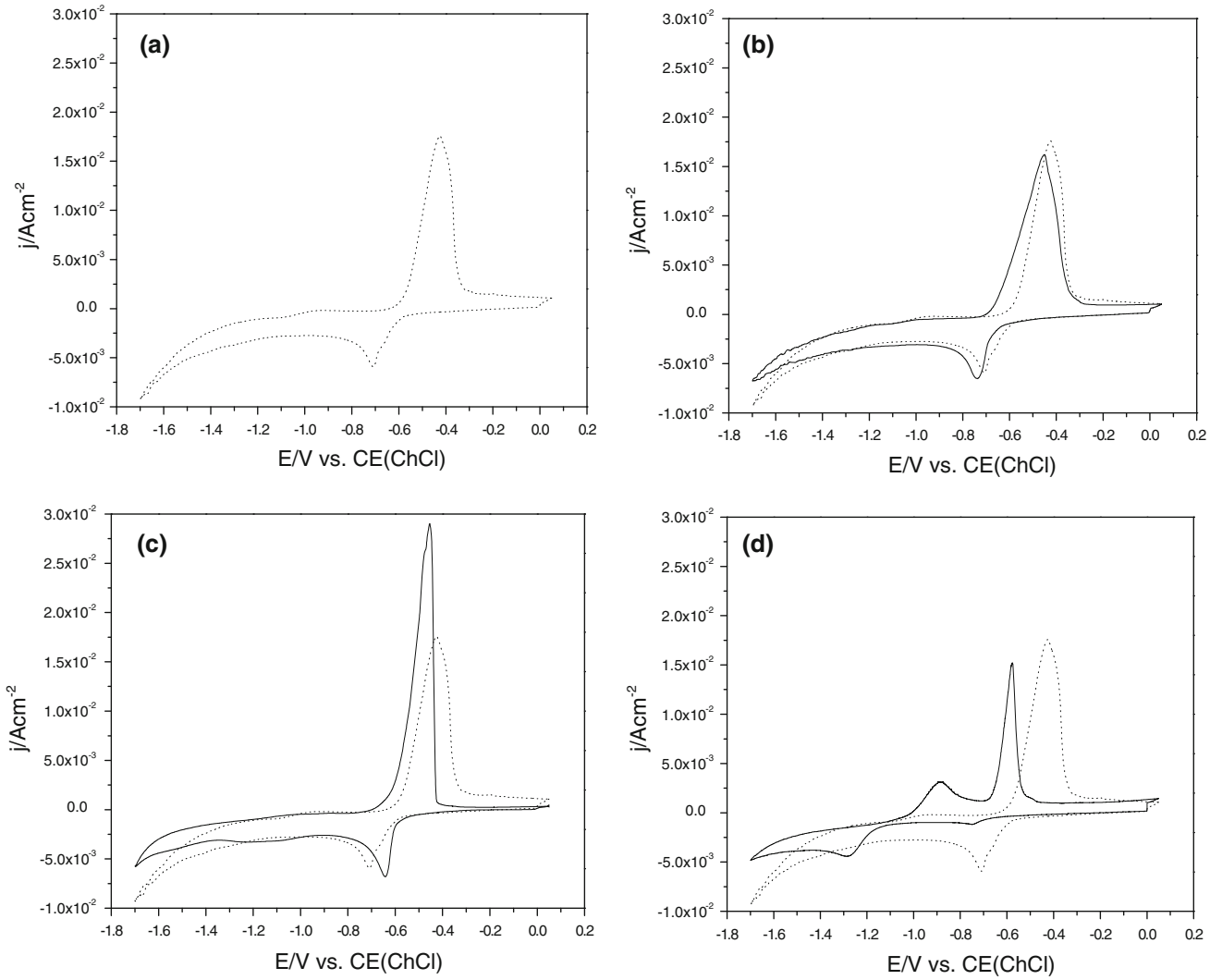

Fig. 3 Cyclic voltammograms for 5.8×10^{-2} M of $SnCl_2$ (**a**) and with the following additives: **b** saturated solution of EDTA, **c** 5.5×10^{-2} M of HEDTA, **d** 5.5×10^{-2} M of Idranal VII using a Pt disk at 75 °C at 50 mVs^{-1} immersed in ethaline. The *dashed lines* in (**b–d**) represent the voltammogram obtained in the absence of additives (**a**)

potential as in the additive-free solution. This may indicate the presence of two Sn species, one complexed with Idranal VII, and the other Idranal VII free. The deposit obtained from these two species originates two oxidative removal processes occurring at two well-separated peak potentials. Both peaks are negatively shifted in relation to the Idranal VII-free solution.

The effect of increasing the concentration of Idranal VII is the decrease of the intensity of the reduction peak corresponding to the reduction of $[SnCl_4]^{2-}$ species and a second reduction peak that occurs at ~ -1.3 V appears. Similarly, the oxidative scan shows a decrease of the main peak at ~ -0.6 V and a second oxidation peak appears at more negative potentials. This is a clear evidence of a competitive complexation process that leads to a second and more stable complex (Sn–Idranal VII) which can only

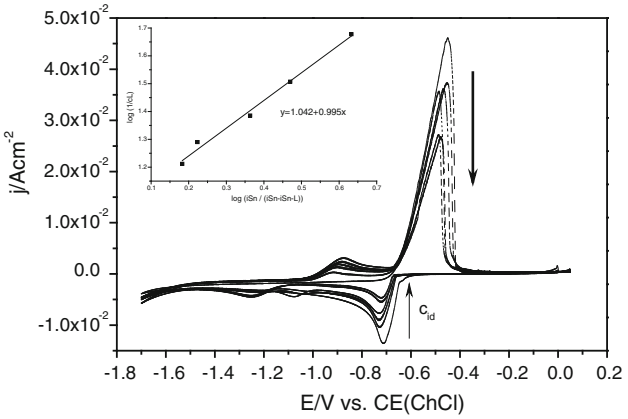

Fig. 4 Cyclic voltammograms for 9.2×10^{-2} M of $SnCl_2$ and increasing concentration of Idranal VII using a Pt disk at 75 °C at 50 mVs^{-1} immersed in ethaline

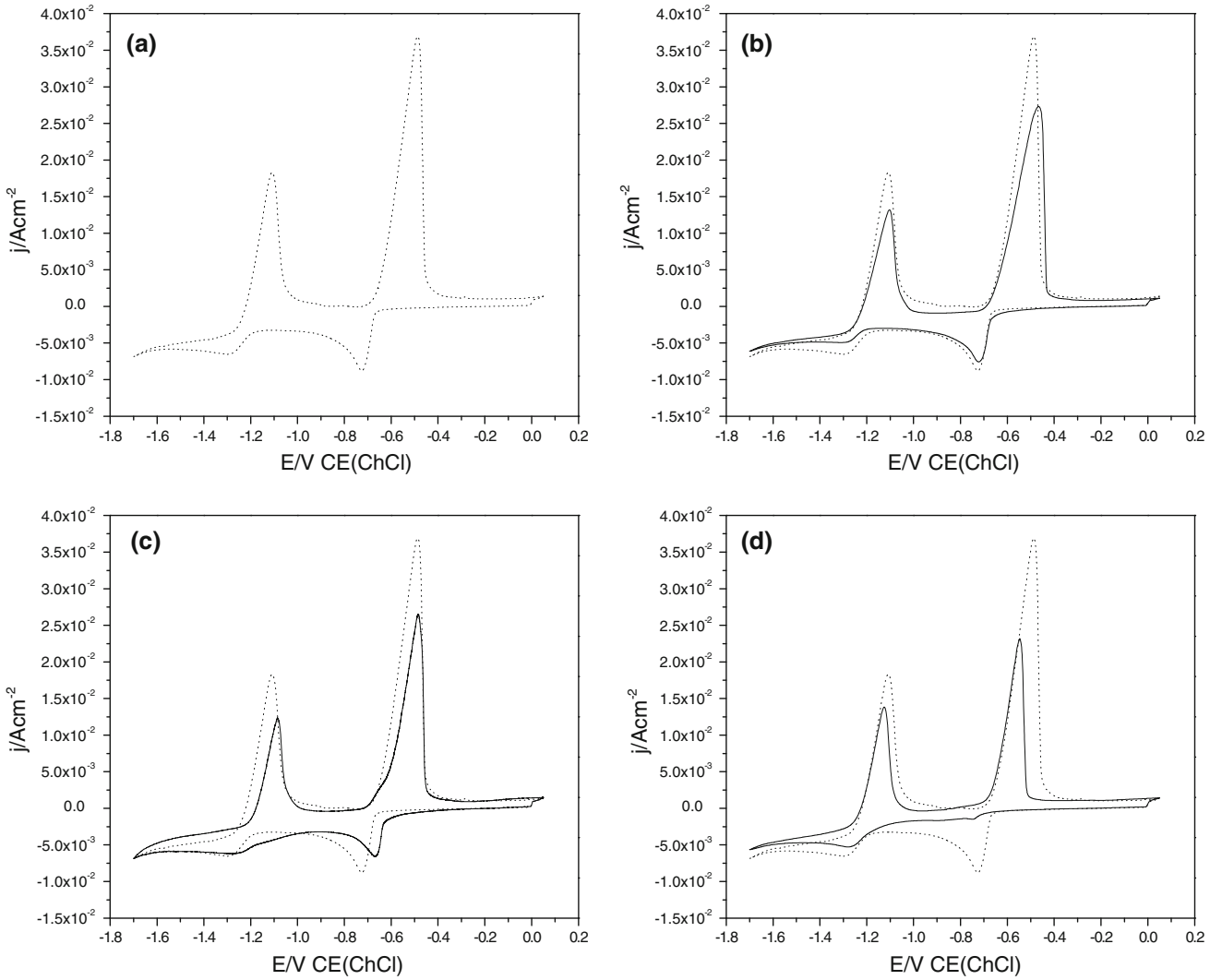

Fig. 5 Cyclic voltammograms for 2.7×10^{-1} M of $ZnCl_2$ and 5.8×10^{-2} M of $SnCl_2$ (**a**) and with the following additives: **b** saturated solution of EDTA, **c** 5.5×10^{-2} M of HEDTA, **d** 5.5×10^{-2} M of Idranal VII using a Pt disk at 75 °C at 50 mVs^{-1} immersed in ethaline. The *dashed lines* in (**b**–**d**) represent the voltammogram obtained in the absence of additives (**a**)

be reduced at more negative potentials (−1.3 V) which is almost coincident with the reduction potential of Zn (II) in the presence of Idranal VII (see Fig. 2d).

Under the assumption of reversible, diffusion-controlled electron transfer and that the complex of Sn (II) with Idranal VII is a 1:1 association complex then this interaction can be described using the Eq. 1:

$$\text{Sn (II)} + \text{Idranal VII} \rightleftharpoons \text{Sn}-\text{Idranal VII} \quad (1)$$

The determination of the apparent binding constant can be calculated using the Eq. 2 [26].

$$\log\left(\frac{1}{C_{\text{Id}}}\right) = \log(K) + \log\left(\frac{i_{\text{Sn}}}{i_{\text{Sn}} - i_{[\text{Sn}-\text{Id}]}}\right) \quad (2)$$

Table 2 Peak potentials (for oxidation and reduction) and CE for zinc and tin co-deposition

	$E_{\text{p ox.}}$ (V) vs. CE(ChCl)		$E_{\text{p red.}}$ (V) vs. CE(ChCl)		CE (%)
	Zinc	Tin	Zinc	Tin	
Additive free	−1.10	−0.48	−1.29	−0.72	83.7
EDTA	−1.10	−0.46	−1.28	−0.72	63.9
HEDTA	−0.94	−0.47	−1.26	−0.66	61.2
Idranal VII	−1.12	−0.54	−1.28	−0.75	69.1

where K is the apparent binding constant, C_{Id} is the concentration of Idranal VII, $i_{[\text{Sn–Id}]}$ is the peak current of Sn (II) after the addition of Idranal VII, and i_{Sn} is the peak

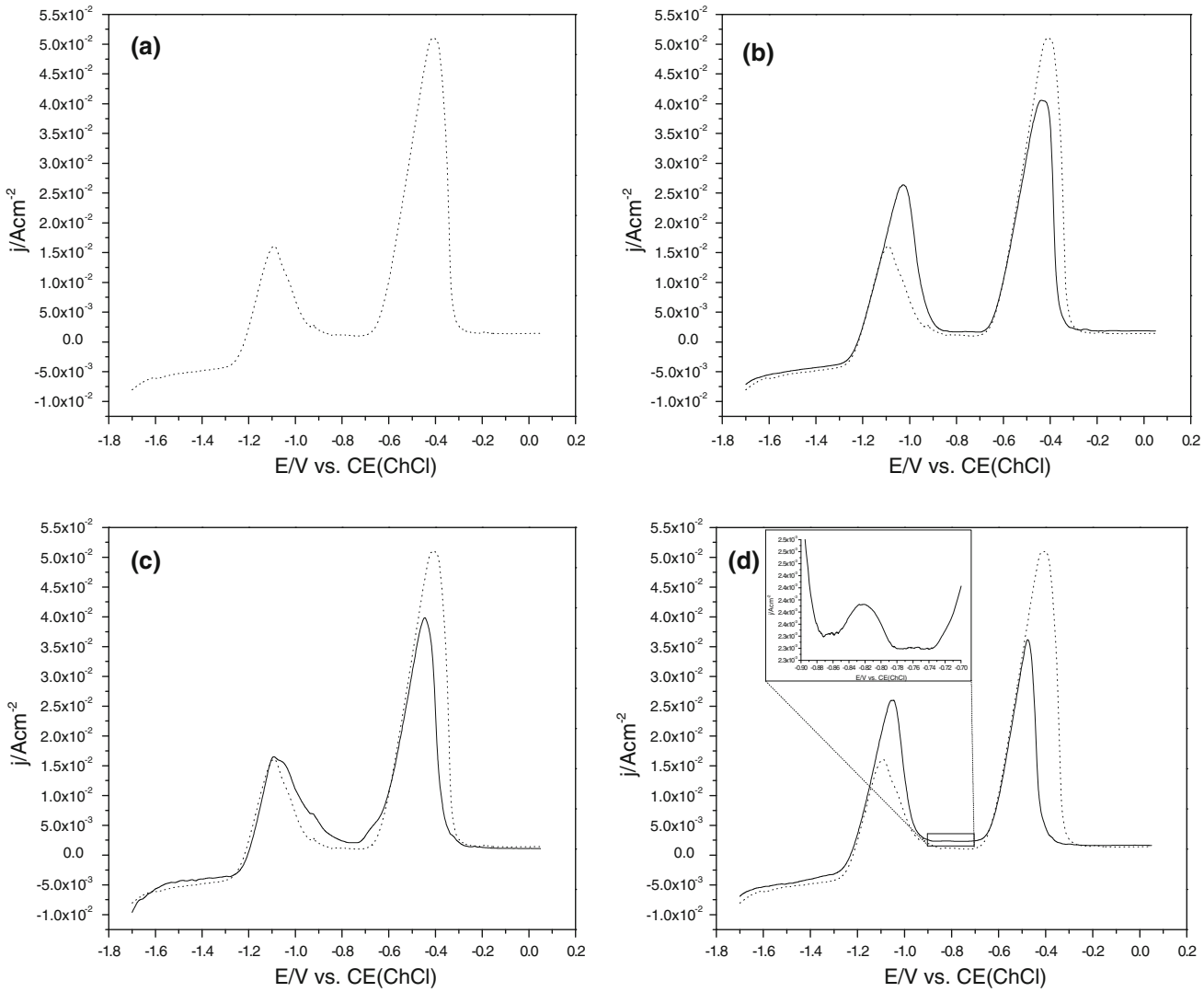

Fig. 6 Striping voltammograms at 50 mVs^{-1} of deposits obtained potentiostatically at −1.7 V on a Pt electrode in ethaline, 2.7×10^{-1} M of $ZnCl_2$ and 5.8×10^{-2} M of $SnCl_2$ (**a**) and with the following additives: **b** saturated solution of EDTA, **c** 5.5×10^{-2} M of HEDTA, **d** 5.5×10^{-2} M of Idranal VII. The *dashed lines* in (**b–d**) represent the voltammogram obtained in the absence of additives (**a**). Deposition time 60 s

current of Sn (II) before the addition of Idranal VII. The plot of $\log(1/C_{Id})$ versus $\log(i_{Sn}/(i_{Sn} - i_{[Sn-Id]}))$ is linear where the intercept is $\log(K)$ (Eq. 2). Figure 4 shows the CV behavior of tin with different concentrations of Idranal VII. Increasing the concentration of the complexing agent with constant tin concentration is observed a decrease of the intensity of the reduction peak. The plot of $\log(1/C_{Id})$ versus $\log(i_{Sn}/(i_{Sn} - i_{[Sn-Id]}))$ is shown in the inset of Fig. 4. According to Eq. 2, the binding constant of this complex is $K = 10.96\ M^{-1}$. The same procedure was repeated using chronoamperometry and the value obtained for the binding constant was $K = 10.71\ M^{-1}$.

3.2.3 Deposition of Zn–Sn

Figure 5a shows the cyclic voltammetric response of an ethaline solution containing a mixture of 2.7×10^{-1} M of $ZnCl_2$ and 5.8×10^{-2} M of $SnCl_2$.

It is clear that the deposition of tin and zinc occurs practically at the same potential as in the individual solution of the metals and therefore the deposition of zinc occurs on tin electrodeposit. The removal of both metals occurs at well-separated potentials with peak potentials similar to those obtained for the isolated metals. These observations are similar to those reported by Abbott et al. [17].

The voltammograms recorded after the addition of the different chelators are shown in Fig. 5b–d. With the exception of the electrodeposition of Zn–Sn in the presence of Idranal VII the $j = f(E)$ profiles in Fig. 5 have similar features, suggesting that the deposition occurs mainly from the same species as in chelator-free solution. As previously mentioned in Sect. 3.2.2, the use of Idranal VII highly suppresses the reduction of Sn at $E \cong -0.7$ V and the reduction of the Sn–Idranal VII complex occurs at $E = -1.28$ V which is overlapped with the reduction of Zn (II).

Table 2 resumes the peak potential for tin and zinc reduction and oxidation and values for the CE.

The CE without additives is larger than in the presence of additives and decreases in the order: Idranal VII > EDTA > HEDTA.

The reduction and oxidation peak potentials vary with the nature of the chelator used as shown in Table 2. In an aqueous solution, the difference between the reduction potential for the two metals is 0.62 V [17], which makes aqueous baths far from ideal to co-deposit Zn (II) and Sn (II) [8]. Changing the aqueous solution with ethaline, the difference between the reduction potential of Sn (II) and Zn (II) is decreased in 40 mV to 0.58 V. A larger effect is obtained when the concentration of Idranal VII is such as to allow the full complexation of Sn (II) in solution; the difference in the Zn (II) and Sn (II) peak potential is very small.

3.2.4 Stripping experiments

Anodic stripping experiments were used to analyze the formation of Sn–Zn deposits. Figure 6 shows the linear stripping curves for the deposits grown potentiostatically with the different additives. The stripping of the metallic deposit shows two distinct peaks with a peak to peak separation of $\cong 600$ mV. In the presence of additives, the Zn (II) stripping peak is larger than in the absence of additives and the area of Sn (II) stripping peak is lower than in the absence of additives. In the case of Sn (II) stripping when Idranal VII is used as additive, it is possible to observe the presence of a small stripping peak at -0.825 V (inset of Fig. 6d) that can be assigned to the oxidation of Sn (II) assisted by Idranal VII complexation as mentioned before.

Assuming the peak assignment made previously in the voltammetric experiments, we can estimate the proportion of zinc and tin in the early stages of the deposit formation by calculating the charge of each oxidation peak.

Figure 7 shows the composition of the deposits obtained in the absence and in the presence of additives. In the absence of additives, the deposits has the composition of 21 % Zn–79 % Sn, that is in the lower limit of zinc in deposit composition pointed as ideal for corrosion purposes. All the additives produce deposits richer in zinc and the largest effect was obtained with the use of Idranal VII (42 % Zn–58 % Sn).

3.2.5 Morphological results

The deposit obtained in the absence of additives (Fig. 8a) is constituted by crystallites with no defined form and seems that the deposit is very porous as reported earlier by

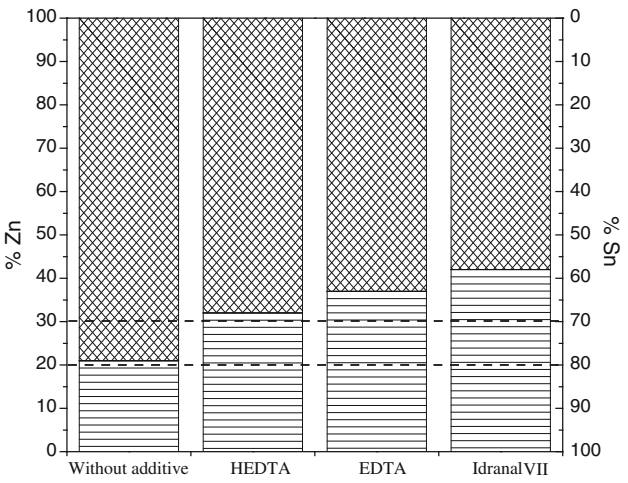

Fig. 7 Proportion of Zn and Sn in the Sn–Zn deposits. The *dashed lines* represent the deposits with composition of 20 % Zn–80 % Sn (*lower line*) and 30 % Zn–70 % Sn (*top line*)

Abbott et al. [17] and can be observed in the inset of Fig. 8a.

The presence of EDTA (Fig. 8b) did not cause any noticeable morphological changes, similar to what was observed with the voltammetric profile. By contrast, using HEDTA (Fig. 8c) leads to a highly irregular deposit which seems to be formed only by crystals with polyhedral shape. Cracks are visible along the deposit.

The effect on the morphology of different concentrations of Idranal VII is illustrated in Fig. 8d, e. When the concentration of Idranal VII is not high enough to complex, all the tin in solution agglomerates are visible on top of an initial layer. Contrasting is the morphology of the deposit obtained when the concentration of Idranal VII exceeds the tin concentration. The deposit covers completely the surface; it is very uniformly distributed with particles of

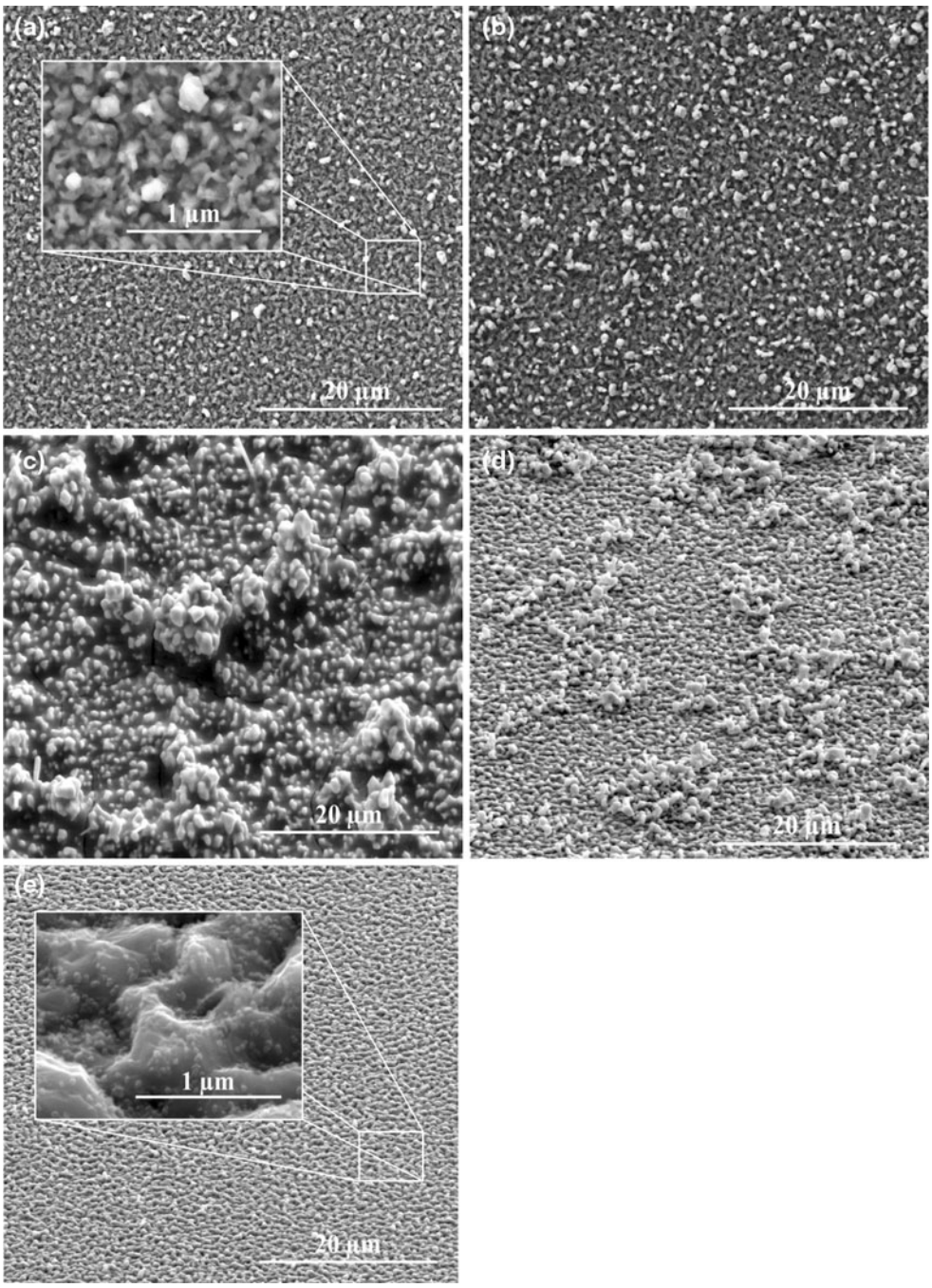

Fig. 8 SEM micrographs of deposits obtained potentiostatically on Pt electrode at $E = -1{,}700$ mV during 600 s in 5.8×10^{-2} M of $SnCl_2 + 2.8 \times 10^{-1}$ M of $ZnCl_2$ solution: **a** without additive; **b** with EDTA; **c** with HEDTA; d with 4.3×10^{-2} M of Idranal VII; **e** with 8.3×10^{-2} M of Idranal VII; **f** EDS analysis of samples (**a**–**d**)

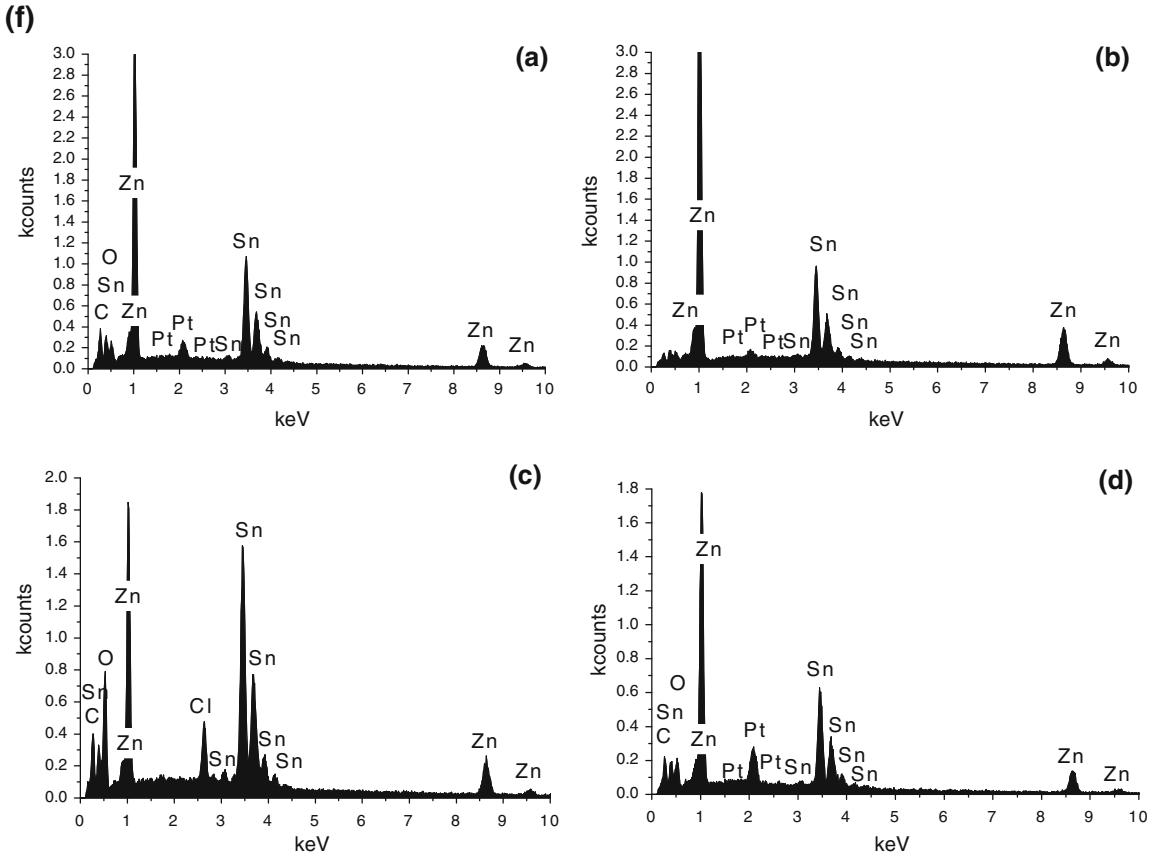

Fig. 8 continued

regular shape. No cracks are detected in the area observed. With higher magnification, it is possible to observe that the particles have quasi spherical shape but on top of them much smaller particles are observed. Similar images were reported by Wang et al. [11].

EDS analysis confirms that all deposits are constituted by zinc and tin as illustrated by Fig. 8f.

4 Conclusions

Zn–Sn deposition could be obtained from DES based on a choline–hydrogen donor mixture. Ethaline was chosen for a more detailed study due to their lower viscosity. For ethaline, the voltammetric results show that morphology and composition of the Zn–Sn electrodeposits is additive dependent.

The highest concentration of zinc in the deposit was obtained using Idranal VII as additive when |Idranal VII| $\geq$ |Sn(II)|. The reason being that Sn (II) complexes selectively with Idranal VII, with an apparent binding constant of $K = 10.96\ \mathrm{M}^{-1}$.

Although HEDTA and Idranal VII ($HEDTANa_3$) have the same molecular backbone, only the fully deprotonated Idranal VII can complex extensively the Sn (II) and in this way changing the electrochemical profile of Sn (II) in ethaline and the morphology of the tin deposits. There is no evidence of the formation of Sn (II) complexes when EDTA or HEDTA are present in the ethaline solution.

When using additives, there is a general trend of increasing CE which can be explained by the reduction of the hydrogen evolution in the presence of the additives. The only exception occurs when zinc is deposit in the presence of HEDTA where the decrease in the CE may be related to the adsorption of HEDTA at the electrode surface impeding the deposition of zinc.

Morphological and chemical characterization of the deposits shows that Idranal VII produces a very uniform zinc-rich deposit.

Acknowledgments The authors wish to thank EU FP6 project IONMET and FP7 project Polyzion for financial support of this study.

References

1. Budman E, Stevens D (1998) Anti-Corros Methods Mater 45:327
2. Taguchi AS, Bento FR, Mascaro LH (2008) J Braz Chem Soc 19:727
3. Guaus E, Torrent-Burgués J (2003) J Electroanal Chem 549:25
4. Chandrasekar MS, Srinivasan S, Pushpavanam M (2010) J Mater Sci 45:1160

5. Dini JW (1995) Electrodeposition. The material science of coatings and substrates. Noyes Publications, Park Ridge
6. Trejo G, Ruiz H, Borges RO, Meas Y (2001) J Appl Electrochem 31:685
7. Oliveira GM, Carlos IA (2009) Electrochim Acta 54:2155
8. Joseph S, Phatak GJ (2010) Mater Sci Eng B 168:219
9. Dubent S, Petris-Wery M, Saurat M, Ayedi HF (2007) Mater Chem Phys 104:146
10. Arici M, Nazir H, Aksu ML (2011) J Alloys Compd 509:1534
11. Wang K, Pickering HW, Weil KG (2001) Electrochim Acta 46:3835
12. Guaus E, Torrent-Burgués J (2005) J Electroanal Chem 575:301
13. Torrent-Burgués J, Guaus E (2007) J Appl Electrochem 37:643
14. Aliaga C, Santos CS, Baldelli S (2007) Phys Chem Chem Phys 9:3683
15. Abbott AP, McKenzie KJ (2008) Phys Chem Chem Phys 8:4265
16. Abbott AP, Boothby D, Capper G, Davies DL, Rasheed RK (2004) J Am Chem Soc 126:9142
17. Abbott AP, Capper G, McKenzie KJ, Ryder KS (2007) J Electroanal Chem 599:288
18. Abbott AP, Ryder KS, Konig U (2008) Trans Inst Met Finish 86:196
19. Whitehead AH, Polzler M, Gollas B (2010) J Electrochem Soc 157:D328
20. Haerens K, Matthijs E, Chmielarz A, Bruggen BV (2009) J Environ Manage 90:3245
21. Endres F, Abbott AP, MacFarlane DR (eds) (2008) Electrodeposition from ionic liquids. Wiley-VCH
22. Kongstein OE, Haarberg GM, Thonsta J (2007) J Appl Electrochem 37:669
23. Abbott AP, Barron JC, Frisch G, Ryder KS, Silva AF (2011) Electrochim Acta 56:5272
24. Abbott AP, Barron JC, Frisch G, Gurman S, Ryder KS, Silva AF (2011) Phys Chem Chem Phys 13:10224
25. Muller C, Sarret M, Andreu T (2002) J Electrochem Soc 149:C600
26. Ibrahim MS (2011) Anal Chim Acta 443:63